Inorganica Chimica Acta 435 (2015) 327–334

Contents lists available at ScienceDirect

Inorganica Chimica Acta

journal homepage: www.elsevier.com/locate/ica

Synthesis and characterization of copper(I) compounds incorporating pyrazole-derived ligands: A study on carbon–carbon coupling reaction

Chen-Yi Li [a], Yu-Ling Lien [a], Jayaramann Vinayagam [a], Amitabha Datta [a], Ting-Chia Hu [a], Chia-Her Lin [b], Jui-Hsien Huang [a,*]

[a] Department of Chemistry, National Changhua University of Education, Changhua 50058, Taiwan
[b] Department of Chemistry, Chung-Yuan Christian University, Chun-Li 320, Taiwan

ARTICLE INFO

Article history:
Received 21 January 2015
Received in revised form 14 July 2015
Accepted 16 July 2015
Available online 22 July 2015

Keywords:
Copper(I)
Pyrazole-derived ligands
Carbon–carbon coupling

ABSTRACT

A series of copper(I) compounds manifesting with the pyrazole mediated precursor, ArN[$CH_2(C_3H_3N_2)$]$_2$ (Ar = 2,6-diisopropylphenyl) (LN3), were synthesized conveniently and treatment of the derivatives with small organic molecules like pyrazine and triphenylphosphine were analyzed. Reacting one and two equivalents of LN3 with $[Cu(CH_3CN)_4]PF_6$ in CH_3CN at room temperature afforded $[Cu(LN3)(CH_3CN)_2]PF_6$ (**1**) and $[Cu(LN3)_2]PF_6$ (**2**), respectively in high yield. Similarly, while reacting one equivalent of LN3 and CuI in acetonitrile for 12 h, produced a white solid, [Cu(LN3)]I (**3**). Furthermore, by adding one or two equivalents of PPh_3 into compound **1**, using methylene chloride as solvent rendered $[Cu(LN3)(PPh_3)]PF_6$ (**4**) and $[Cu(LN3)(PPh_3)_2]PF_6$ (**5**), respectively, in satisfactory yield. In addition, compound $\{[Cu(LN3)(C_4H_4N_2)]_2(PF_6)_2\}_n$ (**6**) was generated as one-dimensional polymer by treating compound **1** and pyrazine in THF at room temperature. All the Cu(I)-derivatives were characterized by ^1H and ^{13}C NMR spectroscopy and the molecular structures (**1**, **4**, and **6**) were determined by single crystal X-ray diffraction. Additionally, the catalytic reactions of Sonogashira type C–C coupling were discussed using compounds **2**, **3**, **5**, and **6** as catalysts.

1. Introduction

Aryl-nitrogen, aryl-oxygen, and aryl-acetylene bonds are prevalent in many compounds that are of pharmaceutical, and materials interest [1,2]. Most noteworthy among them are the aryl coupling reactions based on palladium(0) catalysts such as the Sonogashira coupling [3–5]. Research community has extensively used palladium-based catalysts in cross-coupling reactions in both academic and industrial settings [6]. However, searching non-precious metals as catalysts is also an important issue in development of metal catalyzed C–C coupling reactions. Novel ligand systems and non-precious metal, such as Cu are the two general considered factors for new catalysts. Copper is an important chemical element in the material science [7,8] and organocopper reactions [9–11]. In the past decade, Cu ions are able to shuttle between +1 and +2 oxidation states and making their chemistry useful in the applications of bioinorganic modeling [12–14], oxygen or small molecule activation [15], medicinal chemistry [16], etc. Copper(I) is a highly versatile metal from a coordination standpoint, readily accessing coordination numbers two, three, and four. Its coordinative ability allows copper(I) to play a significant role in many catalytic and stoichiometric processes, including catalytic hydrocarbon functionalization reactions [17]. Copper-catalyzed Sonogashira-type coupling reactions are valuable transformations in organic synthesis [18–22]. Not only Sonogashira reaction, there are many organic reactions were performed with copper [23]. Regarding the ligands of copper catalysts, various chelated nitrogen donor atoms have also been studied and reviewed in the past years [24,25] and some neutral and mono-anionic ligands are shown in Scheme 1. Pyrazoles are extensively used as N-donor ligands to different metal ions [26–28]. The structures and properties of copper pyrazolates are of significant interest which can exhibit a variety of molecular frames with exo-bidentate coordination of the pyrazolate moiety with the copper atoms [29]. Thus, the coordination chemistry of copper incorporating pyrazole-based ligands has drawn recognition because of their interesting unusual structural features, remarkable physical and chemical properties [30–32]. In this connection, we are interested in using bi- or tri-dentate pyrazole ligands to bind Cu atom forming tetrahedral geometry complexes [33–35].

* Corresponding author.
E-mail address: juihuang@cc.ncue.edu.tw (J.-H. Huang).

http://dx.doi.org/10.1016/j.ica.2015.07.018
0020-1693/

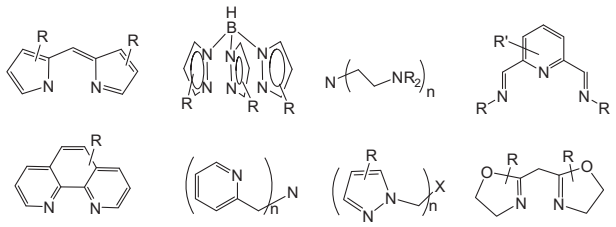

Scheme 1. Neutral and mono-anionic chelated nitrogen donor atoms ligands.

We expand a series of copper(I) compounds coupled with $ArN[CH_2(C_3H_3N_2)]_2$ (Ar = 2,6-diisopropylphenyl) (LN3) and use these derivatives to react with PPh_3 and pyrazine. Compounds **1**–**6** were characterized by ^1H and ^{13}C NMR spectroscopy and most of them were further signalized by single crystal X-ray diffractometry. The catalytic ability of synthesized copper compounds was investigated with Sonogashira type C–C coupling reaction as well.

2. Experimental section

2.1. Materials and physical measurements

All the reactions were performed using standard Schlenk techniques under an atmosphere of high purity nitrogen or in glove box. $Cu(CH_3CN)_4PF_6$, CuI, bis(2-methoxyethyl)amine, formaldehyde and pyrazole (Aldrich) were obtained commercially and used as received. The $ArN[CH_2(C_3H_3N_2)]_2$ (Ar = 2,6-diisopropylphenyl) (LN3) was synthesized according to published literature [23]. All solvents were distilled and stored in solvent reservoir, which contained 4 Å molecular sieves and were purged with nitrogen. ^1H and ^{13}C NMR spectra were recorded on a Bruker Avance 300 spectrometer. Chemical shifts for ^1H and ^{13}C spectra were recorded in ppm relative to the residual protons of $CDCl_3$ (δ 7.24, 77.0). Elemental analyses were performed on a Heraeus CHN-OS Rapid Elemental Analyzer at the Instrument Center of the NCHU.

2.2. Synthesis of the complexes

2.2.1. Synthesis of $[Cu(LN3)(CH_3CN)_2]PF_6$ (**1**)

A 100 mL Schlenk flask charged with $[Cu(CH_3CN)_4]PF_6$ (1.0 g, 2.63 mmol) and 30 mL acetonitrile was added dropwise an acetonitrile solution (30 mL) of LN3 (0.89 g, 2.63 mmol) at 0 °C. The resulting solution was stirred for 12 h and filtered through Celite. The filtrate was vacuum dried and the solid was recrystallized from a toluene/acetonitrile mix solvent to yield white crystals of **1** (1.49 g, 90% yield).^1H NMR ($CDCl_3$): 0.89 (d, 12H, CH*Me*$_2$), 2.20 (s, 6H, C*H*$_3$CN), 2.60 (m, 2H, C*H*Me$_2$), 5.49 (s, 4H, NC*H*$_2$N), 6.29 (t, 2H, pyrazole C*H*), 7.05–7.23 (m, 5H, phenyl C*H* and pyrazole C*H*), 7.74 (d, 2H, pyrazole C*H*). $^{13}C\{^1H\}$ NMR ($CDCl_3$): 2.1 (*C*H$_3$CN), 24.6 (CH*Me*$_2$), 28.4 (*C*HMe$_2$), 73.1 (NCH$_2$N), 106.3 (*C*H, pyrazole), 117.0 (CH$_3$*C*N), 125.0 (*C*H, phenyl), 128.8 (*C*H, pyrazole), 131.4 (*C*H, phenyl), 140.5 (C_{ipso}, pyrazole), 142.4 (C_{ipso}, phenyl), 148.3 (C_{ipso}, phenyl). *Anal.* Calc. for $C_{24}H_{33}CuN_7PF_6$: C, 45.90; H, 5.30; N, 15.60. Found: C, 45.40; H, 5.28; N, 15.70.

2.2.2. Synthesis of $[Cu(LN3)_2]PF_6$ (**2**)

Similar procedure as described for synthesizing **1** was adopted. Ligand LN3 (3.55 g, 10.52 mmol) and $[Cu(CH_3CN)_4]PF_6$ (2.00 g, 5.26 mmol) were used and the resulting solid was recrystallized from a heptane and acetonitrile mix-solvent to generate the colorless solid (4.60 g, 94% yield). ^1H NMR ($CDCl_3$): 1.00 (d, 24H, CH*Me*$_2$), 1.99 (s, C*H*$_3$CN), 2.68 (m, 4H, C*H*Me$_2$), 5.55 (s, 8H, NC*H*$_2$N), 6.36 (t, 4H, pyrazole C*H*), 7.11–7.47 (14H, phenyl and pyrazole C*H*). $^{13}C\{^1H\}$ NMR ($CDCl_3$): 1.7 (*C*H$_3$CN), 24.8 (CH*Me*$_2$), 28.4 (*C*HMe$_2$), 70.9 (NCH$_2$N), 106.8 (*C*H, pyrazole), 116.6 (CH$_3$*C*N), 124.9, 128.7 (*C*H, pyrazole), 130.9, 140.8 (C_{ipso}, pyrazole), 141.1, 148.2. *Anal.* Calc. for $C_{40}H_{54}CuN_{10}PF_6(CH_3CN)_{0.3}$: C, 54.44; H, 6.18; N, 16.11. Found: C, 54.77; H, 6.02; N, 15.11.

2.2.3. Synthesis of [Cu(LN3)]I (**3**)

Similar procedure as discussed for synthesizing **1** was adopted. Ligand LN3 (0.17 g, 0.52 mmol) and CuI (0.10 g, 0.52 mmol) were used and the resulting pale blue solid was recrystallized from an acetonitrile solution to generate the white solid (0.44 g, 81% yield). ^1H NMR ($CDCl_3$): 0.90 (d, 12H, CH*Me*$_2$), 2.60 (m, 2H, C*H*Me$_2$), 5.79 (s, 4H, NC*H*$_2$N), 6.09 (t, 2H, pyrazole C*H*), 7.06–7.27 (m, 5H, phenyl and pyrazole C*H*), 7.97 (d, 2H, pyrazole C*H*). $^{13}C\{^1H\}$ NMR ($CDCl_3$): 24.8 (CH*Me*$_2$), 28.3 (*C*HMe$_2$), 71.7 (NCH$_2$N), 105.0 (*C*H, pyrazole), 124.8, 128.4 (*C*H, pyrazole), 130.1, 141.3 (C_{ipso}, pyrazole), 142.8, 148.6. *Anal.* Calc. for $C_{20}H_{27}N_5CuI$: C, 45.50; H, 5.16; N, 13.27. Found: C, 45.64.; H, 5.23; N, 13.21.

2.2.4. Synthesis of $[Cu(LN3)(PPh_3)]PF_6$ (**4**)

A 100 mL Schlenk flask charged with **1** (1.20 g, 1.91 mmol) and 20 mL methylene chloride was added dropwise with a methylene chloride (20 mL) solution of PPh_3 (0.50 g, 1.91 mmol) at room temperature. The resulting solution was stirred for 12 h and dried under vacuum to yield white solid. The solid was recrystallized from a toluene/methylene chloride solution at −20 °C to generate colorless crystals of **4**. (1.42 g, 92% yield). ^1H NMR ($CDCl_3$): 0.96 (d, 12H, C*H*$_3$), 2.59 (m, 2H, C*H*Me$_2$), 5.60 (s, 4H, NC*H*$_2$N), 6.25 (t, 2H, pyrazole C*H*), 7.09–7.48 (m, 21H, phenyl and pyrazole C*H*). $^{13}C\{^1H\}$ NMR ($CDCl_3$): 24.8 (CH*Me*$_2$), 28.5 (*C*HMe$_2$), 71.9 (NCH$_2$N), 106.9 (*C*H, pyrazole), 125.0, 125.2, 128.2, 128.9, 129.0, 129.4, 130.9, 131.0, 132.2, 133.5, 137.8, 140.5 (C_{ipso}, pyrazole), 143.3, 148.2. *Anal.* Calc. for $C_{38}H_{42}CuN_5P_2F_6(C_6H_5CH_3)_{0.9}$: C, 59.70; H, 5.56; N, 7.86. Found: C, 59.62; H, 5.46; N, 7.72.

2.2.5. Synthesis of $[Cu(LN3)(PPh_3)_2]PF_6$ (**5**)

Similar procedure as mentioned for synthesizing **4** were adopted except that two equivalents of PPh_3 (1.00 g, 3.82 mmol) was used. Complex **5** was obtained from a toluene/methylene chloride solution at −20 °C (1.80 g, 88% yield). ^1H NMR ($CDCl_3$): 1.04 (d, 12H, CH*Me*$_2$), 2.13 (m, 2H, C*H*Me$_2$), 4.89 (s, 4H, NC*H*$_2$N), 6.47 (t, 2H, pyrazole C*H*), 7.04–7.45 (m, 36H, phenyl and pyrazole C*H*). $^{13}C\{^1H\}$ NMR ($CDCl_3$): 25.0 (CH*Me*$_2$), 28.5 (*C*HMe$_2$), 66.1 (NCH$_2$N), 107.8 (*C*H, pyrazole), 124.8, 128.4, 129.0, 130.4, 131.6, 132.0, 133.3, 141.8, 142.4, 147.0. *Anal.* Calc. for $C_{56}H_{57}CuN_5P_3F_6$: C, 62.83; H, 5.37; N, 6.54. Found: C, 62.86; H, 5.31; N, 6.37.

2.2.6. Synthesis of $\{[Cu(LN3)(pyrazine)]_2(PF_6)_2\}_n$ (**6**)

A Schleck flask charged with **1** (0.40 g, 0.64 mmol) and pyrazine (0.051 g, 0.64 mmol) and 30 mL of THF was stirred at room temperature for 12 h. The resulting solution was filtered through Celite and filtrate was concentrated to small volume and stored at −20 °C to afford orange crystals of product (0.10 g, 22% yield). ^1H NMR (d^6-DMSO): 0.91 (d, 12H, CH*Me*$_2$), 2.68 (m, 2H, C*H*Me$_2$), 5.63 (s, 4H, NC*H*$_2$N), 6.40 (t, 2H, pyrazole C*H*), 7.15–7.31 (m, 6H, phenyl C*H*), 7.78 (d, 2H, pyrazole C*H*), 7.89 (d, 2H, pyrazole C*H*), 8.73 (d, 4H, pyrazine C*H*). $^{13}C\{^1H\}$ NMR (d^6-DMSO): 24.4 (CH*Me*$_2$), 27.9 (*C*HMe$_2$), 72.1 (NCH$_2$N), 105.8 (*C*H, pyrazole), 124.7, 128.3 (*C*H, pyrazole), 132.4, 141.3, 141.4, 145.5, 148.1.

2.3. General procedure for C–C bond formation reaction

A glass tube was charged with cesium carbonate (1.0 mmol) and catalyst (5 mol% with respect to the phenylacetylene) and was sealed tightly with rubber septum. The sealed tube was taken out of the glove box and phenylacetylene (2.5 mmol), aryl halide (2.0 mmol) and toluene (15.0 mL) were injected into the tube

through the septum. The septum was changed to glass stopper and the solution was then stirred at 110 °C for overnight. The mixture was then cooled to room temperature and filtered to remove insoluble residues. The filtrate was reduced in vacuo and the residue has taken to GC (Gas chromatography) analysis for separating and analyzing the products that can be vaporized without decomposition.

2.4. Single crystal X-ray structure determination

Single crystals of **1**, **4** and **6** suitable for single crystal X-ray diffractometry analysis were mounted on a Bruker SMART CCD diffractometer equipped with graphite-monochromated Mo K_α radiation (λ = 0.71073 Å). Crystal data were collected at 150 K with an Oxford Cryosystems Cryostream. No significant crystal decay was found. Data were corrected for absorption empirically by means of ψ scans. All non-hydrogen atoms were refined with anisotropic displacement parameters. All the hydrogen atom positions were calculated and they were constrained to idealized geometries and treated as riding where the H atom displacement parameter was calculated from the equivalent isotropic displacement parameter of the bound atom. An absorption correction was performed with the program SADABS [36] and the structures of both complexes were determined by direct methods procedures in SHELXS [37] and refined by full-matrix least-squares methods, on F^2's, in SHELXL [38].

3. Results and discussion

3.1. Synthesis and characterization of complexes *1*–*6*

The synthesis of compounds **1**–**3** is shown in Scheme 2. The pyrazole-derived ligand, $ArN[CH_2(C_3H_3N_2)]_2$ (Ar = 2,6-diisopropylphenyl) (LN3) is synthesized according to literature [23]. Reacting one or two equivalents of LN3 with $[Cu(CH_3CN)_4]PF_6$ in CH_3CN at room temperature generate $[Cu(LN3)(CH_3CN)_2]PF_6$ (**1**) and $[Cu(LN3)_2]PF_6$ (**2**), respectively in high yield. The ^1H NMR spectra of **1** and **2** both show characteristic resonance for the methylene of NCH_2N fragments at δ 5.49 and 5.55, respectively. Compounds **1** and **2** are inter-convertible by adding either LN3 or $[Cu(CH_3CN)_4]PF_6$ as shown in Scheme 2.

Bubbling oxygen to complex **1** in THF, CH_3CN, or CH_2Cl_2 for 3–5 min results color change, from colorless to pale blue, presumably

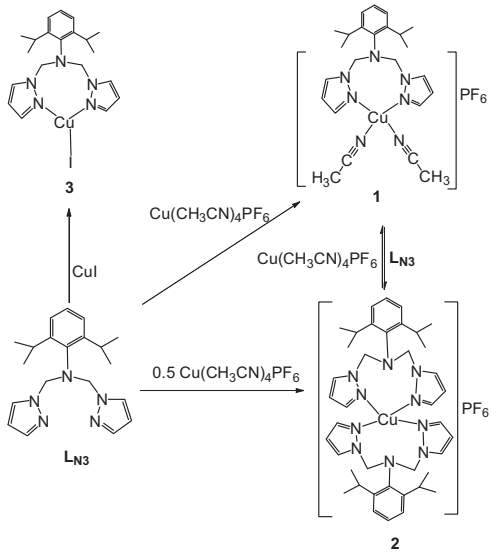

Scheme 2. Synthesis of Compounds **1**–**3**.

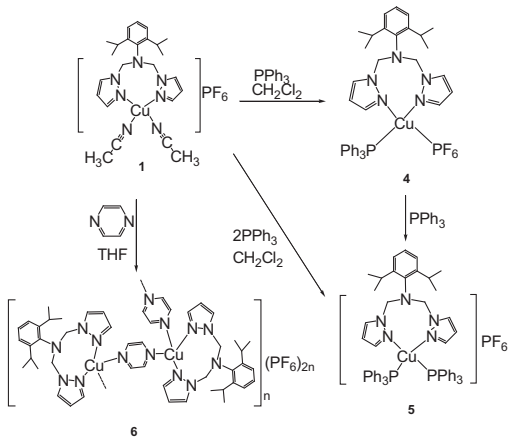

Scheme 3. Synthesis of Compounds **4**–**6**.

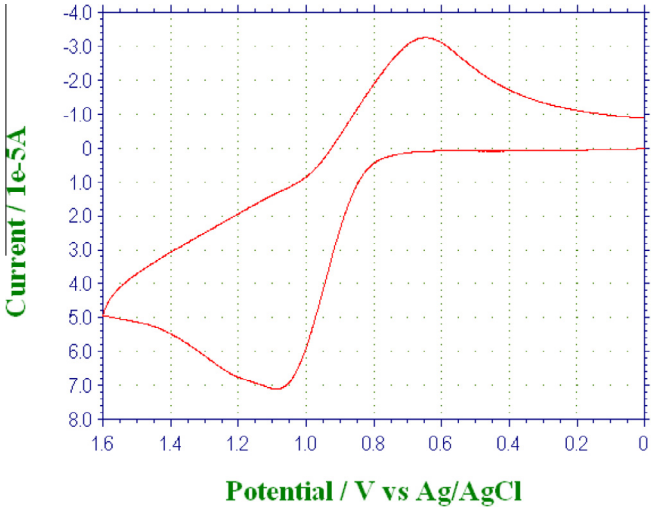

Fig. 1. Cyclic voltammogram of compound **1** in MeCN.

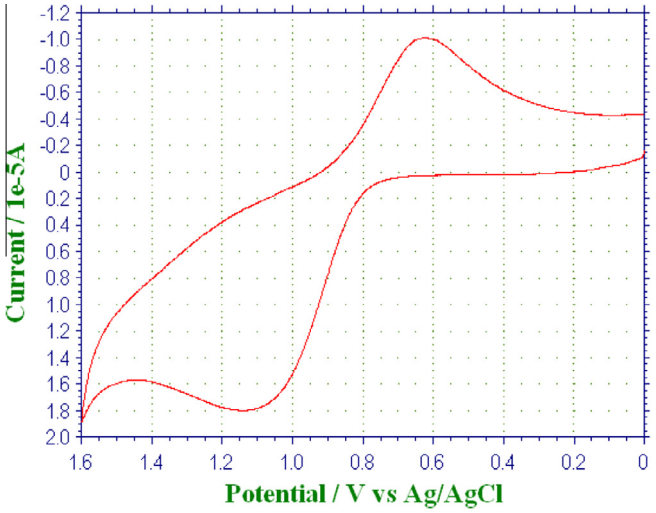

Fig. 2. Cyclic voltammogram of compound **2** in MeCN.

the oxidation state of Cu(I) to Cu(II) in presence of oxygen. However, the ^1H NMR spectrum shows peak broadening due to the formation of paramagnetic d^9 Cu(II) atom. No trace amount

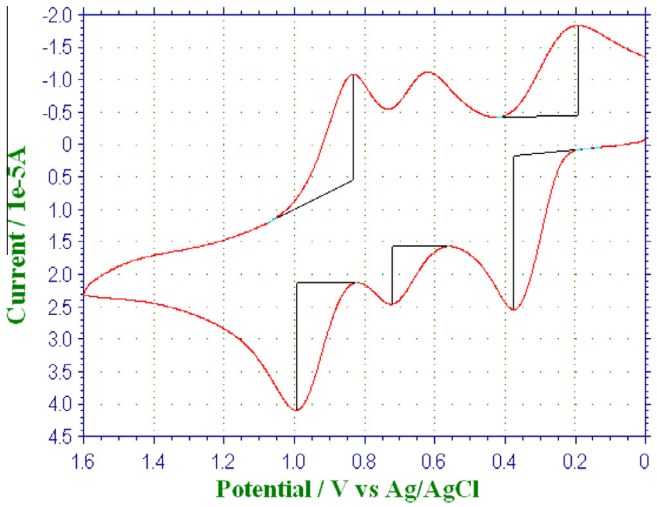

Fig. 3. Cyclic voltammogram of compound **3** in MeCN.

of pure product is isolated from THF or CH_3CN solution. Upon addition of sulfur (S_8) in **1**, no characteristic change is observed. Similarly, during addition of oxygen to **2**, in THF, CH_3CN, or CH_2Cl_2, leads the color change from colorless to pale green; presumably due to Cu(I)/Cu(II) oxidation.

Reacting one equiv of LN3 and CuI in acetonitrile for 12 h generates a white solid, [Cu(LN3)]I (**3**). The ^{1}H NMR spectrum of **3** shows only one methylene resonance at δ 5.79 and one set of CH resonances for the two pyrazole fragments at δ 6.09, 7.12, and 7.97, indicating the symmetrical geometry of compound **3**. On the other hand, when two equivalents of LN3 react with CuI, compound **3** is isolated. But no bis-LN3 Cu compound is observed; presumably due to the large iodine atom prevents the second equiv of LN3 to bind the Cu atom.

The synthesis of compounds **4**–**6** from the reactions of **1** with PPh_3 and pyrazine is shown in Scheme 3. Reacting compound **1** with one or two equivalents of PPh_3 in methylene chloride generates [Cu(LN3)(PPh_3)]PF_6 (**4**) and [Cu(LN3)(PPh_3)$_2$]PF_6 (**5**), respectively. The ^{1}H NMR spectra of **4** and **5** both show characteristic resonance for the methylene group of LN3 ligand at δ 5.60 and 4.89, respectively. Comparing the chemical shifts for the methylene protons among all, compound **5** has a significant upfield shift than those of the others; presumably due to the strong σ donating ability of the PPh_3 groups to enhance the shielding of the methylene protons. Compound **6** is obtained from the reaction of **1** with pyrazine in THF at room temperature for 12 h. Insoluble orange precipitation is filtered off and compound **6**, {[Cu(LN3)(pyrazine)]$_2$(PF_6)$_2$}$_n$, is isolated from the filtrate as only 22% yield. Presumably, high molecular weight of polymeric Cu-pyrazine decreases the yield of **6**. Compound **6** is insoluble in $CDCl_3$, therefore, d^6-DMSO is used as the solvent for ^{1}H and ^{13}C NMR spectra. Again, compound **6** shows a characteristic signal at δ 5.63 and δ 72.1 for the methylene resonance in the ^{1}H NMR and ^{13}C NMR spectra, respectively.

Table 2
The selected bond lengths (Å) and angles (°) for compounds **1**, **4**, and **6**.

1			
Cu(1)–N(7)	1.9971(15)	Cu(1)–N(6)	2.0018(15)
Cu(1)–N(1)	2.0258(14)	Cu(1)–N(5)	2.0364(15)
N(7)–Cu(1)–N(6)	110.73(6)	N(7)–Cu(1)–N(1)	102.38(6)
N(6)–Cu(1)–N(1)	113.46(6)	N(7)–Cu(1)–N(5)	110.09(6)
N(6)–Cu(1)–N(5)	105.04(6)	N(1)–Cu(1)–N(5)	115.24(5)
4			
Cu(1)–N(1)	2.005(1)	Cu(1)–N(5)	2.005(2)
Cu(1)–P(1)	2.212(5)		
N(1)–Cu(1)–N(5)	114.58(7)	P(1)–Cu(1)–F(5)	107.21(5)
N(1)–Cu(1)–P(1)	123.97(5)	N(5)–Cu(1)–P(1)	120.67(5)
6			
Cu(1)–N(14)	1.990(3)	Cu(1)–N(10)	1.999(3)
Cu(1)–N(9)	2.061(3)	Cu(1)–N(8)	2.098(3)
Cu(2)–N(1)	2.004(3)	Cu(2)–N(5)	2.032(3)
Cu(2)–N(6)	2.063(3)	Cu(2)–N(7)	2.110(3)
N(14)–Cu(1)–N(10)	122.75(11)	N(14)–Cu(1)–N(9)	107.93(11)
N(10)–Cu(1)–N(9)	107.67(10)	N(14)–Cu(1)–N(8)	106.96(11)
N(10)–Cu(1)–N(8)	108.94(11)	N(9)–Cu(1)–N(8)	100.30(11)
N(1)–Cu(2)–N(5)	118.55(10)	N(1)–Cu(2)–N(6)	103.99(10)
N(5)–Cu(2)–N(6)	117.34(10)	N(1)–Cu(2)–N(7)	118.43(11)
N(5)–Cu(2)–N(7)	101.25(11)	N(6)–Cu(2)–N(7)	95.60(11)

Table 1
Crystal data and structure refinement for **1**, **4**, and **6**.

	1	**4**	**6**
Formula	$C_{38}H_{49}CuF_6N_7P$	$C_{97}H_{108}Cu_2F_{12}N_{10}P_4$	$C_{56}H_{78}Cu_2F_{12}N_{14}O_2P_2$
Formula weight	812.35	1892.89	1396.34
T (K)	150(2)	150(2)	150(2)
Crystal system	monoclinic	triclinic	orthorhombic
Space group	$P2(1)/c$	$P\bar{1}$	$Pca2(1)$
a (Å)	20.4922(6)	10.9044(3)	19.4601(13)
b (Å)	10.8711(3)	15.3157(4)	10.1541(7)
c (Å)	18.6364(6)	16.2074(7)	32.758(2)
α (°)	90	116.032(2)	90
β (°)	102.523(2)	100.629(2)	90
γ (°)	90	99.4600(10)	90
V (Å^3)	4052.9(2)	2296.37(13)	6472.9(8)
Z	4	1	4
D_c (mg m^{-3})	1.331	1.369	1.433
μ [mm^{-1}]	0.642	0.610	0.793
$F(000)$	1696	986	2896
Reflections collected	42830	43966	68749
Independent reflections (R_{int})	10452 (0.0382)	9853 (0.0231)	16612 (0.0492)
Data/restraints/parameters	10452/0/486	9853/0/573	16612/1/801
Goodness-of-fit (GOF) on F^2	1.060	0.995	1.040
R_1[a], wR_2[b] ($I > 2\sigma(I)$)	$R_1 = 0.0391$, $wR_2 = 0.0997$	$R_1 = 0.0375$, $wR_2 = 0.1031$	$R_1 = 0.0424$ $wR_2 = 0.0997$
R_1[a], wR_2[b] (all data)	$R_1 = 0.0596$, $wR_2 = 0.1068$	$R_1 = 0.0455$, $wR_2 = 0.1081$	$R_1 = 0.0699$ $wR_2 = 0.1150$
Largest difference in peak and hole (e Å^{-3})	0.682 and −0.524	0.692 and −0.565	0.633 and −0.460

[a] $R_1 = \Sigma|F_0| - |F_c|/\Sigma|F_0|$.
[b] $wR_2 = [\Sigma[\omega(F_0^2 - F_c^2)^2]/\Sigma[\omega(F_0^2)^2]]^{1/2}$.

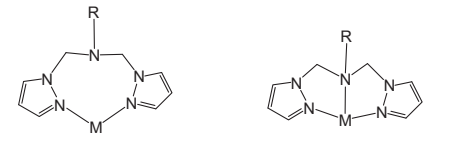

Scheme 4. Possible bonding modes of L_{N3} ligand to metals.

3.2. Cyclic Voltammetry measurements of compounds *1*–*3*

Cyclic Voltammetry studies of compounds **1**–**3** were carried out in 1.0 mM acetonitrile solution belonging the potential range between 0 V and 1.6 V. While increasing and decreasing the voltage, simultaneously the oxidation and reduction process advances showing an oxidation (E_{pa}) and reduction peak (E_{pc}), respectively. Therefore, the cyclic voltammetry studies provide the information of the oxidation/reduction potential of the new compounds. All solutions were prepared in the glove box and the measurements were carried out under nitrogen atmosphere. The Cyclic Voltammetry spectra of compounds **1**–**3** are shown in Figs. 1–3. The Cyclic Voltammetry of **1** shows an anodic peak (E_{pa}) at +1.09 V and a cathodic peak (E_{pc}) at +0.65 V. The ΔE_p and the current peak ratio of these two peaks are as expected for a irreversible Cu(II)/Cu(I) system. Similarly, complex **2** shows an anodic peak (E_{pa}) at +1.14 V and a cathodic peak (E_{pc}) at +0.62 V. The ΔE_p and the current peak ratio of these two peaks are also as expected for a irreversible Cu(II)/Cu(I) process. The oxidation process for both **1** and **2** correspond at high anodic peak (E_{pa}) than those of similar compounds in literature [24,25], presumably due to weak donating ability of neutral LN3 ligand that causes the difficulty of Cu(I)/Cu(II) oxidation.

Three reversible redox peaks of the cyclic voltammetry spectrum of **3** are observed and their $E_{1/2}$ values are at +0.28 V (E_{pa} = +0.37 V, E_{pc} = +0.19 V), +0.67 V (E_{pa} = +0.72 V, E_{pc} = +0.62 V), and +0.91 V (E_{pa} = +0.99 V, E_{pc} = +0.82 V). Presumably, compound **3** in solution is not only in a three coordinated monomeric format; but the solvent and counter anion may also bind the Cu atom making the redox spectrum more complicate (*vide infra*).

3.3. Molecular structures of compounds *1*, *4*, and *6*

The crystal data of compounds **2** and **5** were collected; however, the data is not good enough for publication and so, their structures were not discussed in this paper. The summary of crystal data collection for compounds **1**, **4**, and **6** and their selected bond lengths and angles are listed in Table 1 and 2, respectively. LN3 ligand binds to metals in two possible modes as shown in Scheme 4 involving type (a) N,N,-κ^2-LN3 mode and type (b) N,N,N,-κ^3-LN3 mode. However, all the molecular geometries of the compounds in this paper act as type (a) N,N,-κ^2-LN3 model. The crystals of **1** were obtained from a saturated acetonitrile solution at −20 °C and its molecular geometry is shown in Fig. 4. Complex **1** adopts a four coordinate tetrahedral geometry with four nitrogen donor atoms, one pair each from pyrazole-N fragments and acetonitrile-N molecules. The LN3 ligand binds to the Cu atoms through two pyrazole fragments forming an eight-member ring. The 2,6-diisopropylphenyl ring and the two acetonitrile molecules are located in a plane which dissects the LN3–Cu eight-member ring, as shown in Fig. 5. The biting angle of N(1)–Cu(1)–N(5) is 115.24(5)°, larger than the angle of tetrahedral geometry, presumably due to the large ring constraint of the eight-member ring. The bond lengths of Cu atom to the N atoms of two pyrazole fragments are at 2.026(14) Å and 2.036(15) Å, consistent with the literature [39,40]. The bond lengths of Cu(I) atom to acetonitriles associate also in normal range (*ca.* 2.00 Å) as reported before [41–43]. The anionic PF_6 belongs outside the Cu coordination sphere where the Cu–P_{PF6} bond length is longer than 5.0 Å indicating no interaction between the two ionic molecules.

The colorless crystals of **4** were obtained from a saturated toluene/methylene chloride solution at −20 °C. There are eight molecules in unit cell, but only one molecule is considered for molecular discussion. The geometry of **4** is depicted in Fig. 6. The central Cu(I) atom is surrounded by two pyrazole-N atoms and one triphenylphosphine P atom. The Cu–$N_{pyrazole}$ and Cu–P_{PPh3}

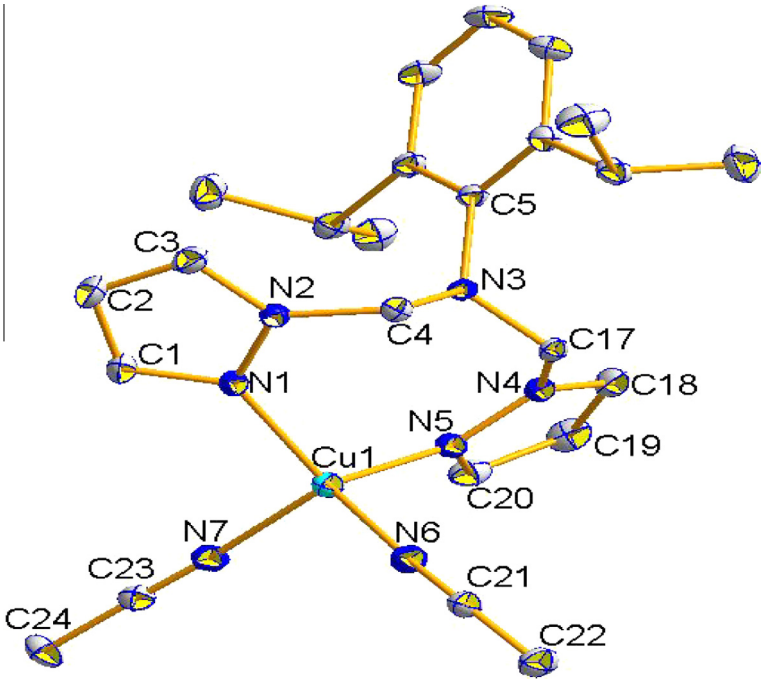

Fig. 4. The molecular structure of compound **1**, thermal ellipsoids were drawn at 30% probability. The toluene molecules, PF_6, and all hydrogen atoms are omitted for clarity.

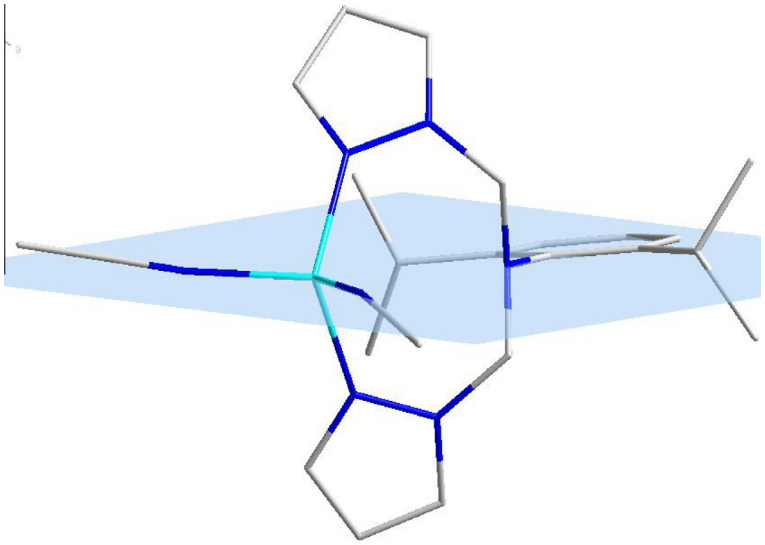

Fig. 5. A perspective view of compound **1** through the phenyl ring, Cu atom and two acetonitrile molecules.

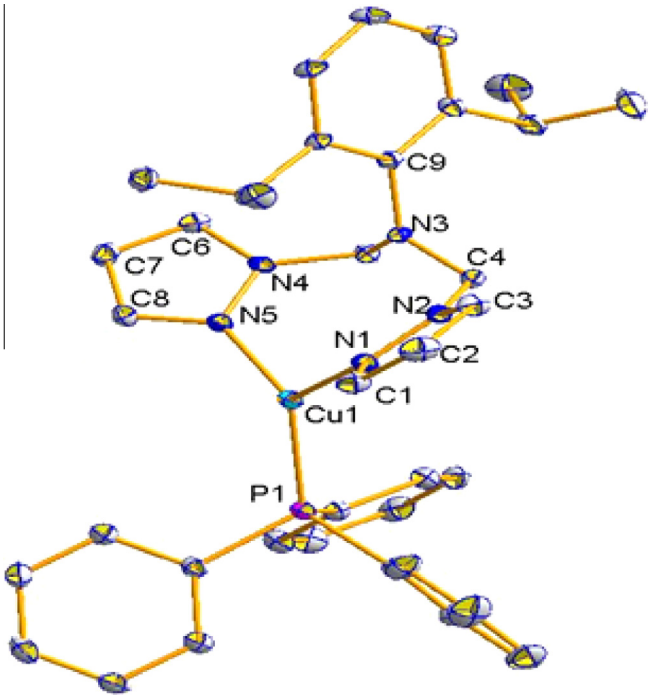

Fig. 6. The molecular geometry of compound **4**, thermal ellipsoids were drawn at 30% probability. The hydrogen atoms are omitted for clarity.

bond lengths are similar as in complex **1**; *i.e.* 2.00 Å and 2.21 Å, respectively [44,45]. Several aspects are worthy to emphasize the crystal structure of **4**. The molecular geometry can be viewed as a trigonal plane being considered as a cation. The Cu(I), P(1), N(3), atoms and the phenyl ring may be arranged in a plane which also bisects the eight-membered chelate ring (see Fig. 7).

The orange crystals of **6** were obtained from a saturated THF solution at −20 °C and its molecular geometry is shown in Fig. 8. The central Cu(I) atom is surrounded by two donor pyrazole-N atoms of LN3 ligand and a pair of bridging N atoms from two different units of pyrazine molecules. The geometry around Cu(I) lies on an inversion center can be conveniently described as a tetrahedron. The metal ion thus exhibits in a CuN4 coordination mode

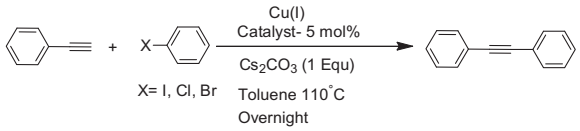

Scheme 5. C–C coupling of phenylacetylene and aryl halide using Cu(I) catalysts.

Table 3
Conversion rate of the formation of diphenylacetylene from phenylacetylene and arylhalide*.

	Complex **2**	Complex **3**	Complex **5**	Complex **6**
I	98	95	98	98
Br	97	99	99	99
Cl	no reaction	trace	trace	trace

* Conversion rate of formation of diphenylacetylene from phenylacetylene and arylhalide in % were calculated through GC analysis.

showing a distorted tetrahedral geometry. The distortion of the structures from square planar to tetrahedral can be evaluated through the parameter Δ introduced by Galy et. al. [46] and applied by Ribas and Kahn [47]. Deviations of atoms from the least-squares plane through N(5), N(6), N(7) and N(1) atom is 0.24 Å. Thus the angles, N(6)–Cu(2)–N(7) and N(1)–Cu(2)–N(5) for Cu2 and N(10)–Cu(1)–N(14) and N(8)–Cu(1)–N(9) for Cu1 are greater than the ideal value of 90°. The *trans* angles, N(1)–Cu(2)–N(7) and N(5)–Cu(2)–N(6) for Cu2 and N(8)–Cu(1)–N(10) and N(1)–Cu(1)–N(9) deviate from the ideal bond angle 180°. The Cu–$N_{pyrazole}$ bond lengths, ranging from 1.990 to 2.032 Å, are well comparable with previous molecular structures. The bridging pyrazine-N atoms connect each copper(I) ion to two neighbouring ones (the Cu...Cu separation distance is 6.973 Å), generating an infinite zig-zag one-dimensional chain.

*3.4. Carbon–Carbon coupling catalytic reaction for compounds **2**, **3**, **5** and **6***

Four compounds were chosen for the Sonogashira type C–C coupling reaction. For test and optimization of the reaction

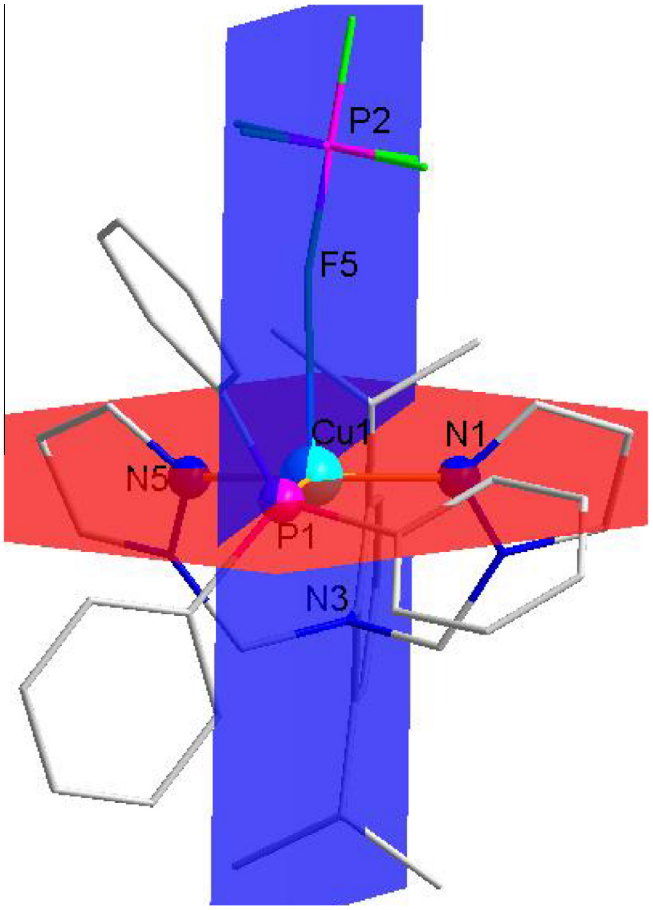

Fig. 7. The perspective view of **4** showing the Cu atom is located on the center of the N(1), N(5), and P(1) trigonal plane (plane in red) and Cu(I), P(1), N(3), and the phenyl ring are arranged in a plane and bisect the chelated eight-member ring (plane in blue). (For interpretation of the references to color in this figure legend, the reader is referred to the web version of this article.)

conditions, we used the standard reaction technique (toluene, 110 °C, K_2CO_3 as base) described in literature [48]. Herein, we selected Cs_2CO_3 as base to obtain best result among K_2CO_3 and Et_3N. These reactions were performed with cesium carbonate (1.0 mmol), catalyst (5 mol% with respect to the phenylacetylene (2.50 mmol)), aryl halide (2.00 mmol) and toluene (15.0 mL). The contents were then stirred at 110 °C for overnight under N_2 atmosphere (Scheme 5). Final products of these reactions, diphenylacetylene and their corresponding derivatives were analyzed by gas chromatography. The diphenylacetylene peak exactly matches with authentic diphenylacetylene peak in GC. These results are summarized in Table 3. In our reaction conditions aryl chloride is not reactive compared to aryl iodide and aryl bromide may be due to the differences in bond energy between aryl iodides (ca. 65 kcal/mol) and aryl bromides (ca. 81 kcal/mol) [49]. Aryl iodides and bromides are generally much more reactive than chlorides; depending upon dissociation energies of aryl halides (for Ph–I, Ph–Br and Ph–Cl, 280, 346 and 407 kJ mol^{-1}, respectively) and can readily be employed in the chemical reactions, with iodides being more reactive due to the weaker C–I bond [50]. The corresponding bromides and especially chlorides are less prone to participate, requiring more forcing conditions [51,52], the extent to which depends upon levels of halide activation and specifics of ligand choice. It employs a copper catalyst to form a carbon–carbon bond between a terminal alkyne and an aryl halide. During the course of the reaction, the presence of base results in the formation of a pi-alkyne complex, which makes the terminal proton on the alkyne more acidic, leading to the formation of the copper acetylide. Then it continues to react with the intermediate to regenerate the copper halide. Further development of the reaction with more metal derivatives and other C–N, C–O bond formation reaction in under investigation.

4. Conclusion

In summary, a series of copper(I) compounds with a pyrazole based N-donor precursor and corresponding derivatives with small organic molecules were analyzed. Single crystal X-ray diffraction

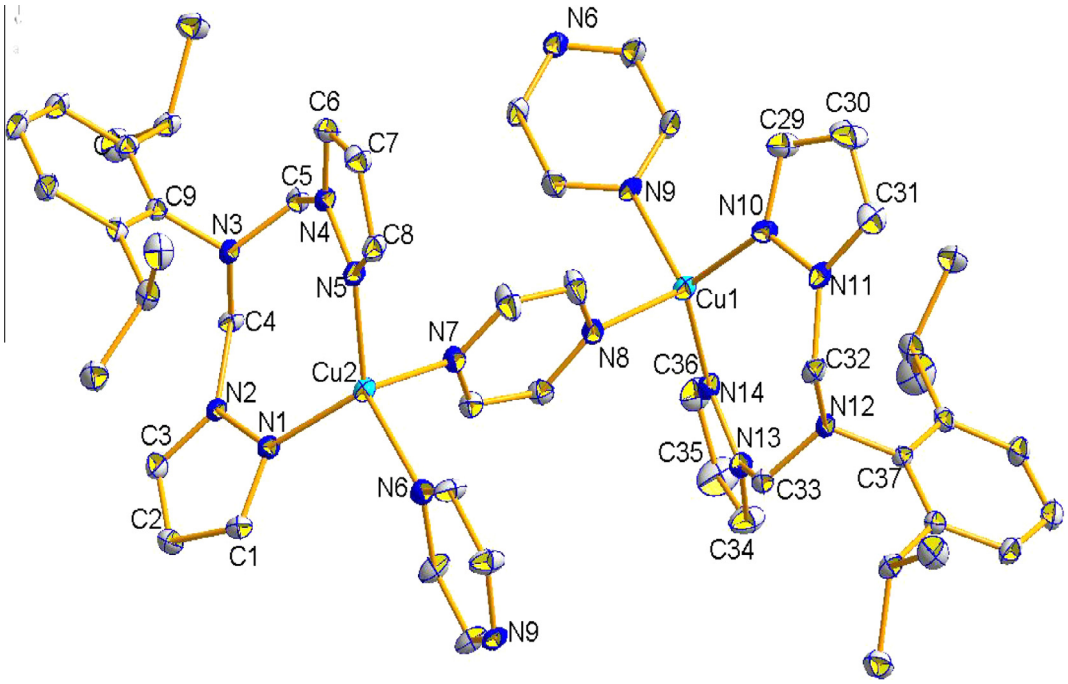

Fig. 8. The molecular geometry of **6**, thermal ellipsoids were drawn at 30% probability.

study confirms that the central Cu atom possesses on a distorted tetrahedron in compounds **1**, **4** and **6**. Cyclic voltammetry study is well consistent to determine the redox potential of Cu(II)/Cu(I) system. The Sonogashira type coupling reactions show that the I and Cl substituents have better conversion rate for the formation of diphenylacetylene from phenylacetylene and aryl halide using Cu(I) derivatives as catalyst. Future work will explore the design of new substituted pyrazole ligands and study the reactivity with copper(I)-derivatives inserting as well different organic molecules.

Acknowledgments

We acknowledge the financial assistance from the Ministry of Science and Technology of Taiwan. We would also like to thank the National Changhua University of Education for providing the facility of X-ray diffractometer and NMR spectrometer.

Appendix A. Supplementary material

CCDC 1035923–1035927 contain the supplementary crystallographic data for this paper. These data can be obtained free of charge from The Cambridge Crystallographic Data Centre via www.ccdc.cam.ac.uk/data_request/cif. Supplementary data associated with this article can be found, in the online version, at http://dx.doi.org/10.1016/j.ica.2015.07.018.

References

[1] H.B. Goodbrand, N.-X. Hu, J. Org. Chem. 64 (1999) 670.
[2] Y. Hong, G.J. Tanoury, H.S. Wilkinson, R.P. Bakale, S.A. Wald, C.H. Senanayake, Tetrahedron Lett. 38 (1997) 5607.
[3] J.F. Hartwig, Syn. Lett. 4 (1996) 329.
[4] G. Mann, J.F. Hartwig, Tetrahedron Lett. 38 (1997) 8005.
[5] M.S. Driver, J.F. Hartwig, J. Am. Chem. Soc. 119 (1997) 8232.
[6] G. Floris, B. Mondovi (Eds.), Copper Amine Oxidases: Structures, Catalytic Mechanisms, and Role in Pathophysiology, CRC Press, 2010.
[7] U. Landau (Ed.), The Bactericidal and Oligodynamic Action of Silver and Copper in hygiene, Medicine and Water Treatment, RSC, 2007.
[8] "The Chemistry of Organocopper Compounds: Part 1 and 2", Z. Rappoport, I. Marek, Ed., 2009, John Wiley & Sons Ltd.
[9] J.T. Rogers, D.K. Lahiri, Curr. Drug Targets 5 (2004) 535.
[10] J. Zhang, F. Zhang, H. Li, C. Liu, J. Xia, L. Ma, W. Chu, Z. Zhang, C. Chen, S. Li, Curr. Med. Chem. 19 (2012) 2957.
[11] S.G. Kaler, Neurology 7 (2011) 15.
[12] S.V. Ley, A.W. Thomas, Angew. Chem., Int. Ed. 42 (2003) 5400.
[13] A. Caballero, M.M. Diaz-Rodriguez, T.R. Belderrain, M.C. Nicasio, S. Trofimenko, P.J. Perez, J. Am. Chem. Soc. 125 (2003) 1446.
[14] W. Kirmse, Angew. Chem., Int. Ed. 42 (2003) 1088.
[15] A. Meijere, 2nd ed., in: F. Diederich (Ed.), Metal-Catalysed Cross-Coupling Reactions, Wiley-VCH, Weinheim, 2004.
[16] C.C.C.J. Seechurn, M.O. Kitching, T.J. Colacot, V. Snieckus, Angew. Chem., Int. Ed. 51 (2012) 5062.
[17] W.-W. Chan, Z. Zhou, W.-Y. Yu, Chem. Commun. 49 (2013) 8214.
[18] C. Zarate, R. Martin, J. Am. Chem. Soc. 136 (2014) 2236.
[19] A.R. Thomas, Z. Baoguo, S. Yian, Tetrahedron Lett. 51 (2010) 1822.
[20] B.H. Lipshutz, S. Huang, W.W.Y. Leong, G. Zhong, N.A. Isley, J. Am. Chem. Soc. 134 (2012) 19985.
[21] T. Thaler, P. Knochel, Angew. Chem., Int. Ed. 48 (2009) 645.
[22] H.Z. Liang, J.J. Adam, Z. Erik, B. Carsten, Chem. Eur. J. 19 (2013) 8144.
[23] C.-Y. Li, Y.-L. Lien, A. Datta, W.-T. Chiu, C.-L. Hsu, J.-H. Huang, L. Horng, C.-H. Lin, C.-J. Su, J. Chin. Chem. Soc. 59 (2012) 696.
[24] C.C. Chou, C.C. Su, A. Yeh, Inorg. Chem. 44 (2005) 6122.
[25] K. Fujisawa, T. Ono, Y. Ishikawa, N. Amir, Y. Miyashita, K.I. Okamoto, N. Lehnert, Inorg. Chem. 45 (2006) 1698.
[26] S. Trofimenko, Chem. Rev. 93 (1993) 943.
[27] R. Mukherjee, Coord. Chem. Rev. 203 (2000) 151.
[28] S. Muñoz, J. Pons, J. Ros, C.A. Kilner, M.A. Halcrow, J. Organomet. Chem. 696 (2011) 2736.
[29] M.K. Ehlert, S.J. Rettig, A. Storr, R.C. Thompson, J. Trotter, Can. J. Chem. 68 (1990) 1444.
[30] A.L. Gavrilova, B. Bosnich, Chem. Rev. 104 (2004) 349.
[31] E. Bouwman, W.L. Driessen, J. Reedijk, Coord. Chem. Rev. 104 (1990) 143.
[32] V. Mishra, F. Lloret, R. Mukherjee, Eur. J. Inorg. Chem. (2007) 2161.
[33] E. Kim, H.Y. Woo, S. Kim, H. Lee, D. Kim, H. Lee, Polyhedron 42 (2012) 135.
[34] W.L. Driessen, F.B. Hulsbergen, J. Reedijk, G.C. Verschoor, Transition Met. Chem. 10 (1985) 390.
[35] A. Panella, J. Pons, J. Garcia-Anton, X. Solans, M. Font-Bardia, J. Ros. Inorg. Chim. Acta 359 (2006) 4477–4482.
[36] SADABS, Area-Detector Absorption Correction; Bruker AXS Inc.: Madison, WI, 2004.
[37] G.M. Sheldrick, SHELX97- Programs for Crystal Structure Analysis: Structure Determination (SHELXS), University of Göttingen, Germany, 1997.
[38] G.M. Sheldrick, SHELX97- Programs for Crystal Structure Analysis: Refinement (SHELXL), University of Göttingen, Germany, 1997.
[39] S.S. Massoud, M.C. Lamieux, L. Le Quan, R. Vicente, J.H. Albering, F.A. Mautner, Inorg. Chim. Acta 388 (2012) 71.
[40] L. Zhang, Z.-G. Ren, H.-X. Li, J.-P. Lang, Cryst. Eng. Comm. 13 (2011) 1400.
[41] J.M. Knaust, S.W. Keller, Cryst. Eng. Comm. 5 (2003) 459.
[42] S. Nieto, V.M. Lynch, E.V. Anslyn, H. Kim, J. Chin, J. Am. Chem. Soc. 130 (2008) 9232.
[43] D. Ferraris, B. Young, C. Cox, W.J. Drury III, T. Dudding, T. Lectka, J. Org. Chem. 63 (1998) 6090.
[44] K. Fujisawa, S. Chiba, Y. Miyashita, K. Okamoto, Eur. J. Inorg. Chem. (2009) 3921.
[45] D.L. Reger, B. Reinecke, M.D. Smith, R.F. Semeniuc, Inorg. Chim. Acta 362 (2009) 4377.
[46] J. Galy, J.J. Bonner, S. Anderson, Acta Chem. Scand. A33 (1979) 383.
[47] J. Ribas, C. Diaz, R. Costa, Y. Journaux, C. Mathoniere, O. Kahn, A. Gleizes, Inorg. Chem. 29 (1990) 2042.
[48] R.K. Gujadhur, C.G. Bates, D. Venkataraman, Org. Lett. 3 (2001) 4315.
[49] L. Djakovitch, P. Rollet, Adv. Synth. Catal. (2004) 1782.
[50] R.A. Batey, M. Shen, A.J. Lough, Org. Lett. (2002) 1411.
[51] M. Alami, F. Ferri, G. Linstrumelle, Tetrahedron Lett. 34 (1993) 6403.
[52] Z. Novak, A. Szabo, J. Repasi, A. Kotschy, J. Org. Chem. 68 (2003) 3327.